Electronic Supplementary Material (ESI) for Nanoscale.

Supporting Information

Sonoelectrosynthesis of Monodisperse Metal Nanoparticles

Kelly K. Rudman,[a] Seyyedamirhossein Hosseini,[a,b] Kaustav Chatterjee,[a] Benjamin Johnson,[a,c] and Sara E. Skrabalak[a*]

[a] *Department of Chemistry, Indiana University, Bloomington, IN 47405, USA*

[b] *Department of Chemistry, The University of Utah, Salt Lake City Utah 84112, USA*

[c] *Department of Chemistry, Purdue University, West Lafayette, IN 47907, USA*

*Corresponding author: sskrabal@indiana.edu

.

Table of Contents

Electrochemical Setup

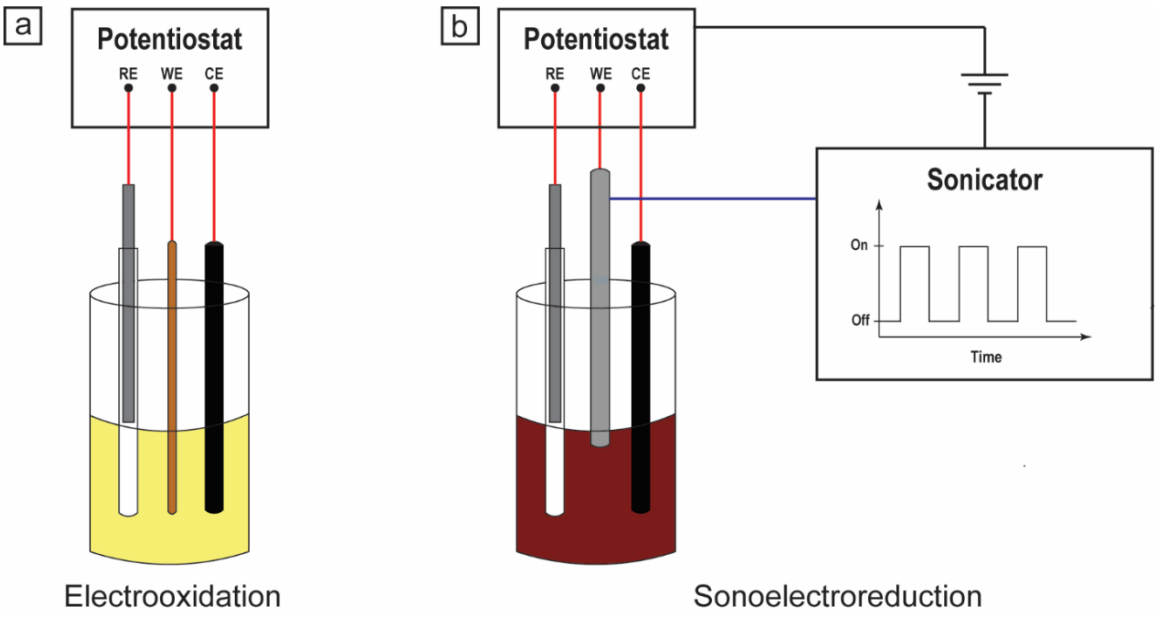

Figure S1. Electrochemical cell set up for (a) electrooxidation and (b) sonoelectroreduction.

Determination of Electrolyte and Surfactant

Many NPs syntheses use reverse micelles to maintain size and shape control. Toluene and water is a common solvent system for these type of syntheses. However, toluene has a low dieletric constant of 2.38,[1] which makes it unable to conduct a sufficient current to quickly synthesize nanoparticles. To create an adequate reverse micelle for electrosynthesis the solvent system must meet the following conditions: (1) two immiscible solvents must be present, (2) both solvents must be able to conduct electricity, (3) the organic phase must make up most of the composition. It was determined that a suitable solvent system consisted of 97.7:2.3 CH_3NO_2: H_2O (ε_{CH3NO2}=38 ε_{H2O}=80).[2, 3]

Determination of Critical Micelle Concentration via Capillary Electrophoresis.[4]

Methods. The critical micelle concentration of CTAB in a 97.7:2.3 CH_3NO_2–H_2O medium was determined via the micellar electrokinetic chromatography (MEKC) mode on an Agilent HP G1600AX 3D capillary electrophoresis system equipped with a 40 cm × 75 μm bared fused-silica CE capillary (Agilent). The capillary was flushed at 930 mbar with 20 mM borate (pH = 9.3) buffer for 3 min. Afterwards, 0–100 mM CTAB solutions were flushed at 930 mbar for 3 min. A potential of 15 kV was applied for 5 min and the average current recorded. This procedure was repeated with the addition of 10, 100, and 340 mM CTAB in 97.7:2.3 CH_3NO_2–H_2O.

Discussion. Since a reverse micelle template is used to synthesize Cu NPs, it is necessary to determine the CMC of CTAB in the 97.7:2.3 CH_3NO_2/H_2O solvent system used during synthesis. This is so enough surfactant is in solution to form the reverse micelle. Common methods to determine CMCs are UV-Vis spectroscopy and conductivity titrations. However, common dyes and copper sulfate are not soluble in the present solvent system, which prevents absorbance measurements and therefore UV-Vis spectroscopy cannot be used. A conductivity titration was unable to be performed due to the low sensitivity of the available conductivity probe to detect small changes in conductivity upon addition of CTAB. Previous works have shown that CMCs can be determined via the CE mode, micellar electrokinetic chromatography (MEKC).[5, 6] The analyte can be separated into its various components by charge via application of an electric potential to the CE capillary.[7] To determine the CMC, the current of the 97.7:2.3 CH_3NO_2/H_2O was recorded with increasing concentrations of CTAB (Figure S1).

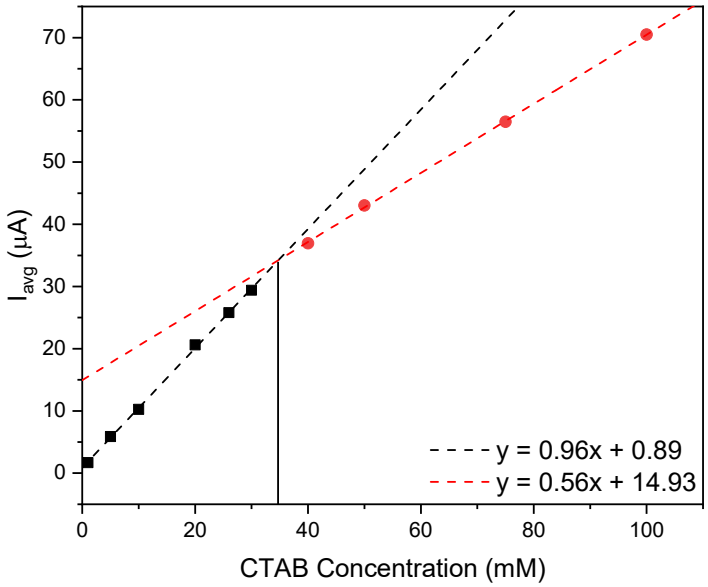

Figure S2. Determination of critical micelle concentration of CTAB in 97.7:2.3 CH_3NO_2:H_2O via MEKC in the absence of HCl. Potentials were held at 15 kV.

Note that CTAB was selected as the surfactant due to its solubility in CH_3NO_2. As the concentration of CTAB increased, there is a linear increase in current. When the CMC is reached, there is a decrease in the slope. This is due to the positively-charged surfactant molecules forming a spherical micelle, which will travel slower through the capillary due to its larger size, thus increasing the frictional force, and due to the positive charges being shielded by hydrophobic tails, thus decreasing the pull from the electric field applied across the capillary.[8] In the absence of HCl, the CMC of CTAB in 97.7:2.3 CH_3NO_2:H_2O was 35 mM (Figure 1).

The addition of acid is necessary to activate the Cu wire for electrooxidation and prevents the copper ions from being reduced at the counter electrode by introducing the competitive HER reaction. Upon addition of 10 mM acid, the CMC decreases to approximately 23 mM CTAB, and there is no significant shift in the CMC upon further addition of acid (Table S1). This shift in CMC can be attributed to addition of protons in solution, which decreases the charge density of the ammonium head groups, thereby increasing the stability of the micelle at lower

concentrations.[9] However, once the acid is added to the medium, there is no longer a decrease in the CMC as the extent of hydrogen-bonding will no longer increase. It is also of significance that the concentration of HCl cannot surpass 340 mM or else coacervation occurs, where the medium will separate into colloid-rich and colloid-deficient phases due to the increased hydrogen-bonding at lower pHs.[10] From these results, it was decided that copper NPs would be synthesized in the presence of 50 mM CTAB. This concentration is beyond that of the CMC, so additional surfactant molecules form more micelles, but below the solubility limit of CTAB in CH_3NO_2.

Table S1. Critical micelle concentrations of CTAB in 97.7:2.3 CH_3NO_2:H_2O determined via micellar electrokinetic chromatography.

HCl Concentration (mM)	CMC (mM)
0	35.1
3.75	22.9
37.5	22.0
125	25.3

Role of CTAB

Cu NPs were synthesized at 20% intensity, $\eta = -59$ mV, $t_{pulse} = 1$ s, and $t_{rest} = 5$ s in the absence of CTAB (Figure S6). These NPs formed dendritic assemblies; therefore, CTAB is necessary to ensure all NPs are spherical.

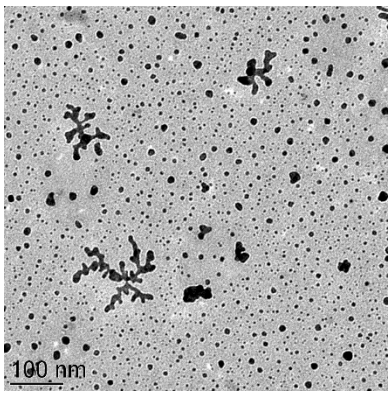

Figure S3. Transmission electron micrograph of Cu NPs synthesized in the absence of CTAB at 20% intensity, $\eta = -59$ mV, $t_{pulse} = 1$ s, and $t_{rest} = 5$ s.

Reference Electrode Preparation

As the solvent for electrosynthesis of metallic nanoparticles is comprised of mainly CH_3NO_2, a new reference electrode must be prepared in CH_3NO_2 to avoid the formation of a liquid junction potential.[11] and allow for accurate reports of the applied potential. Herein, we describe the preparation of a Ag/AgCl in 0.05 M TMACl in CH_3NO_2.

A Ag/AgCl quasi-reference electrode was made by electroplating AgCl onto an Ag wire. The Ag wire was immersed in a 1 M HCl and a constant current 100 mA for 20 min. The electrode was then rinsed with deionized water followed by CH_3NO_2 and then placed into a glass tube equipped with a porous tip (CH111, CH Instruments, Inc.) containing a 0.05 TMACl–CH_3NO_2. This reference electrode was allowed to equilibrate for approximately 1 week or until a steady open circuit potential was obtained. Open circuit potential experiments were performed in a previously described cell[12] with the Ag/AgCl in 0.05 M TMACl–CH_3NO_2 as the working electrode, saturated calomel electrode as the reference, and 0.05 M TMACl–CH_3NO_2 as the electrolyte. The open circuit potential between the 2 electrodes was recorded over the course of 1 h and 3 h (See Figure S3). The open circuit potential was determined to be –34 ± 3 mV . The deviation falls within the acceptable range of ±5 mV for reference electrodes.[13] Therefore, the prepare electrode can be used for electrolysis. Note, as the electrolysis involves sonication, the reference potential was measured before and after experiments to check the stability. If the reference potential drifted more than 5 mV the reference electrode was allowed to equilibrate before running additional experiments.

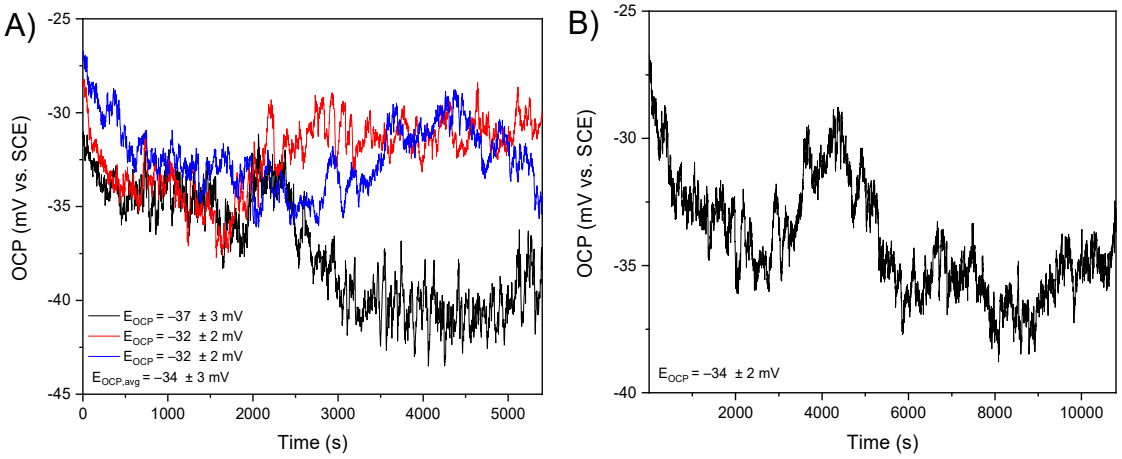

Figure S4. Open circuit potential measurements for a Ag/AgCl reference electrode 0.05 M TMACl–CH_3NO_2 vs. SCE. Experiments were performed for a duration of (a) 1 h and (b) 3 h.

Sonic Probe Calibration

A Branson SFX150 Sonifier was calibrated via a calorimetry experiment. Distilled H_2O (50 mL) was place into a dewer with a styrofoam lid, which contained a hole to place the sonic probe into H_2O. The initial temperature was recorded for 3 min. The sonic probe then continuously sonicated at a constant intensity for 15 min. The temperature was recorded during sonication and for 12 min afterwards (Figure S3A). The power output of the sonic probe was then calculated with the following equation (Figure S3B):[14, 15]

$$P = \frac{dT}{dt} C_{P,H_2O} m_{H_2O}$$

where P is power output (W), $\frac{dT}{dt}$ is change in temperature over time (° C/s), C_{P,H_2O} is the specific heat capacity of water (4.184 J/ (g*°C)), and m_{H_2O} is the mass of water (g).

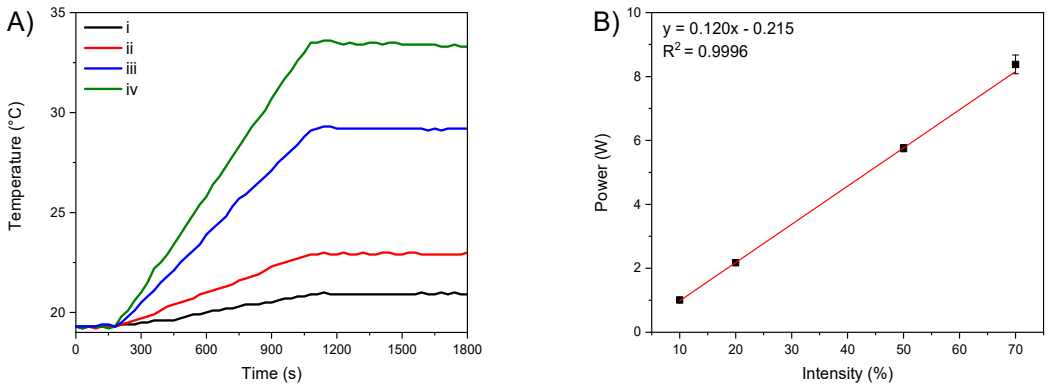

Figure S5. Calorimetric curves to determine power output of sonic probe (A) and corresponding calibration curve (B). Measurements were recorded at 10% (A.i., black), 20% (A.ii., red), 50% (A.iii., blue), 70% (A.iv., green).

Electrosynthesis Variables

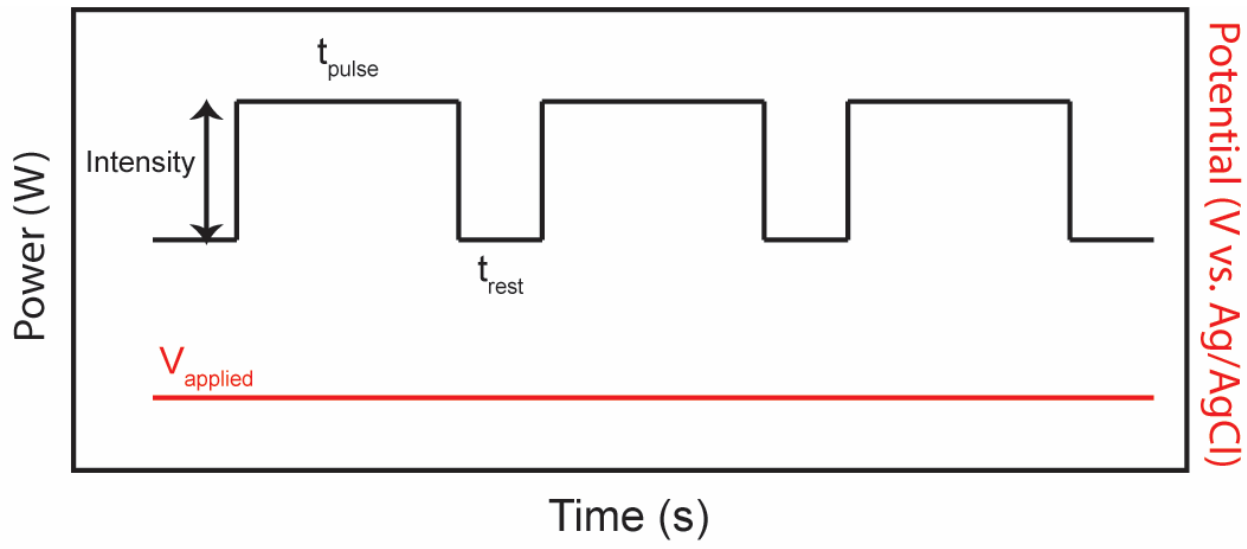

Figure S6. General schematic of ultrasonic horn operation during NP synthesis. Variables that to be investigated include: applied potential ($V_{applied}$), sonication intensity, and pulse duration (t_{pulse}/t_{rest}).

X-ray Photoelectron Spectroscopy

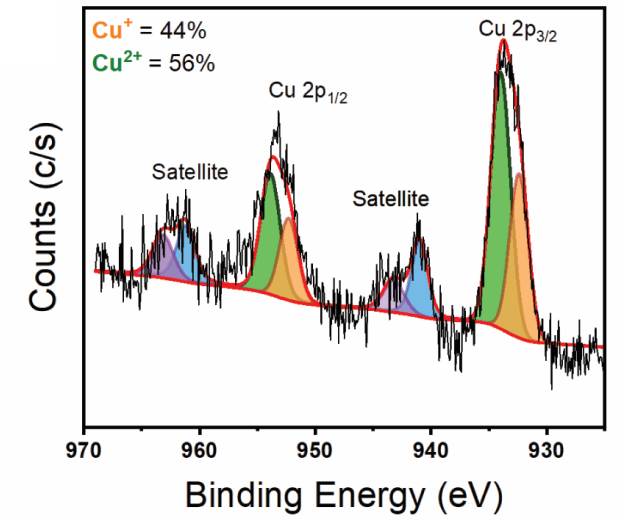

Figure S7. X-ray photoelectron spectrum for oxidized copper solution. Peaks at 932.3 eV and 952.3 eV correspond to $2p_{3/2}$ and $2p_{1/2}$ of Cu^{2+}, respectively. Peaks at 934.1 eV and 953.9 eV correspond to $2p_{3/2}$ and $2p_{1/2}$ of Cu^{2+}.

Cyclic Voltammetry

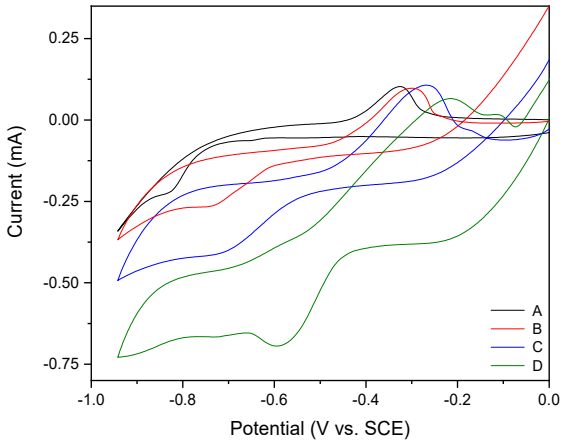

Figure S8. Cyclic voltammograms of 10 mM (A, black), 25 mM (B, red), 50 (C, blue), and 100 mM (D, green) $CuBr_2$ in oxygen-free 0.05 M TMACl–CH_3NO_2 containing 50 mM CTAB and 100 mM $CuBr_2$ recorded at planar 308 stainless steel disk electrode (area = 0.071 cm^2). Voltammograms were obtained at 25 mV s^{-1}; scans go from 0.0 to –0.95 V vs. Ag/AgCl (0.05 TMACl–CH_3NO_2) with a potential of –34 mV vs. SCE at 25 ºC.

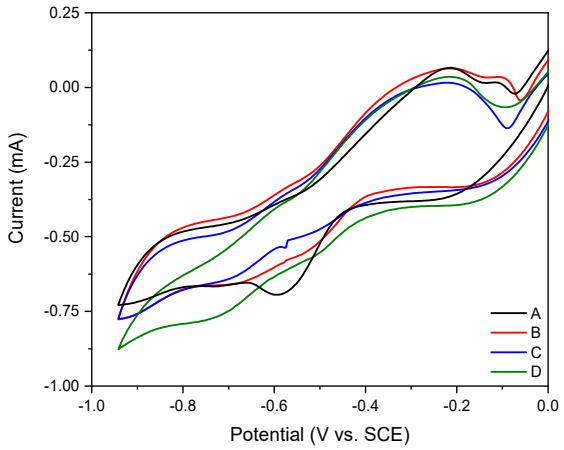

Figure S9. Cyclic voltammograms of 0 mM (A, black), 25 mM (B, red), 50 (C, blue), and 100 mM (D, green) HCl in oxygen-free 0.05 M TMACl–CH_3NO_2 containing 50 mM CTAB recorded at planar 308 stainless steel disk electrode (area = 0.071 cm^2). Voltammograms were obtained at 25 mV s^{-1}; scans go from 0.0 to –0.95 V vs. Ag/AgCl (0.05 TMACl–CH_3NO_2) with a potential of –34 mV vs. SCE at 25 ºC.

Cyclic voltammetry of $CuBr_2$ was performed in 0.05 M TMACl–CH_3NO_2 containing 50 mM CTAB with the use of the Ag/AgCl QRE in 0.05 M TMACl in CH_3NO_2 (Figure S5). However, CV potentials are reported with respect to SCE. $CuBr_2$ was selected as the analyte rather than introduction of Cu^{2+} to easily control the precursor concentration rather oxidation of Cu^0 metal into solution. As the solution also contains Br^- from CTAB, $CuBr_2$ is an appropriate salt to describe the electrochemical behavior of the Cu^{2+} solution used for sonoreduction. Addition of TMACl is necessary to increase the conductivity of the solution so that current signal may be detected before the addition of HCl. The reduction of Cu^{2+} to Cu^0 was determined to be approximately –0.55 V vs. SCE with an onset potential of –0.38 V vs. SCE. All potentials are reported with respect to this onset potential. Upon addition of HCl, the $Cu^{2+/0}$ peak becomes less apparent as HER also occurs. Despite the presence HER, Cu reduction still occurs during sonoelectroreduction as a constant potential experiment is implemented. Furthermore, HCl was incrementally added to determine whether acid concentration significantly shifted peak potential (Figure S6). It was shown that the

addition of acid resulted in a less pronounced peak which is attributed to the increase of HER that can occur.

Powder X-ray Diffraction

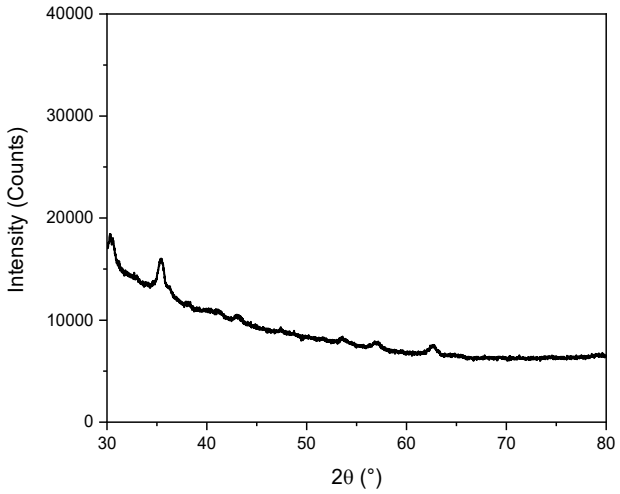

Figure S10. Powder X-ray diffactogram of Cu NPs. These reflections do not correspond to common copper-containing phases and are likely arise from excess surfactant in the sample.

High Resolution Transmission Electron Microscopy

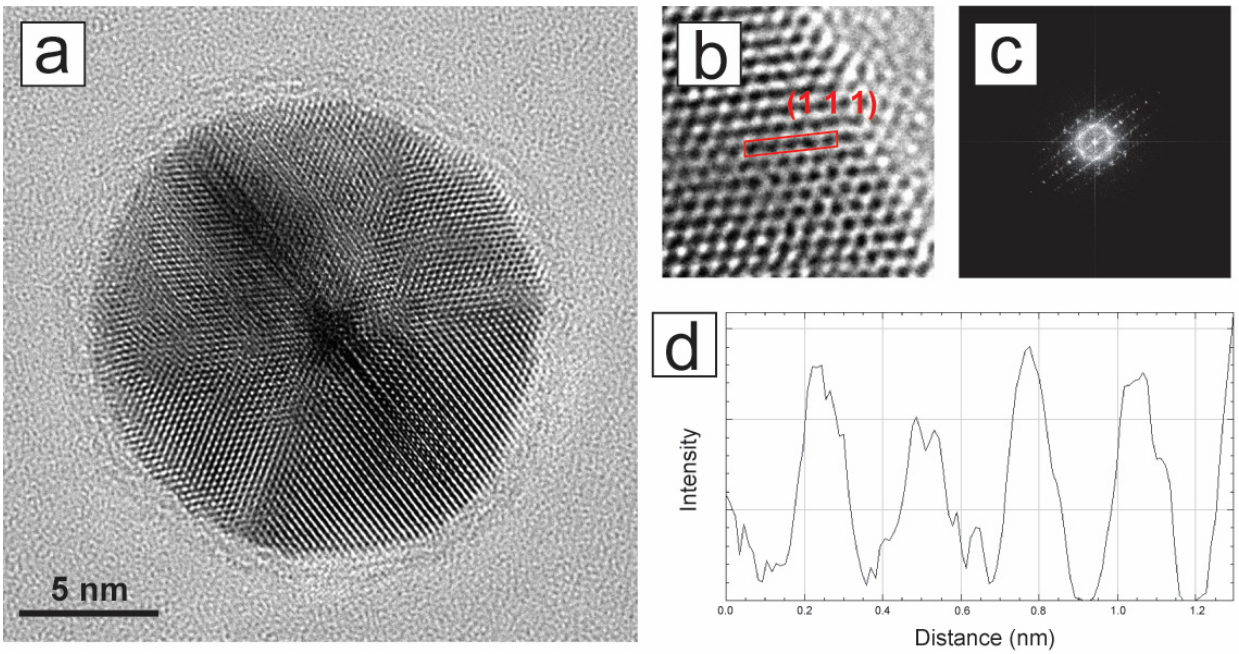

Figure S11. (a) High resolution TEM image of a Cu NP. (b) enlarged image (a) depicting imaged lattice fringes. (c) FFT of individual nanoparticle. (d) Intensity profile from the red box shown in (b).

Energy Dispersive X-ray Spectroscopy

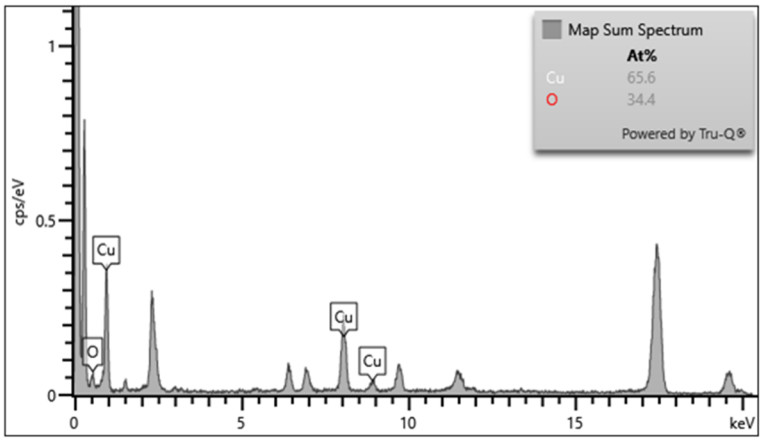

Figure S12. Energy-dispersive X-ray spectroscopy map sum spectrum.

Without Applied Potential

Cu NPs were synthesized at 20% intensity, t_{pulse} = 1 s, and t_{rest} = 5 s in the absence of an applied potential (Figure S7). Note that Cu will spontaneously deposit on Fe. Therefore, Cu NPs are formed despite no applied potential. However, the NPs appear to be larger in size.

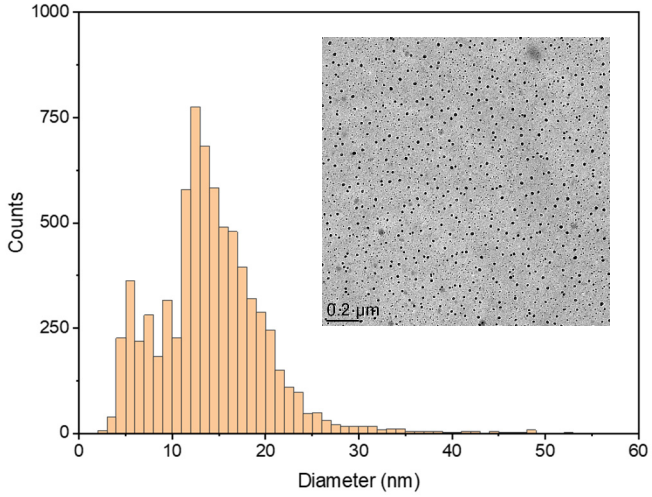

Figure S13. Transmission electron micrograph and corresponding size distribution of Cu NPs synthesized at 20% intensity, t_{pulse} = 1 s, and t_{rest} = 5 s in the absence of an applied potential.

Nanoparticle Size Distributions.

Shown below are the size distributions for all nanoparticle syntheses. All distributions are fitted with a bigaussian distribution as NPs are so small such that the particle will dissolve back into solution if the diameter is sufficiently small.

Table S2. Cu NPs Distribution for Applied Potentials.*				
$V_{applied}$ (mV)	Distribution	Peak 1 (nm)	Peak 2 (nm)	Peak 3 (nm)
80	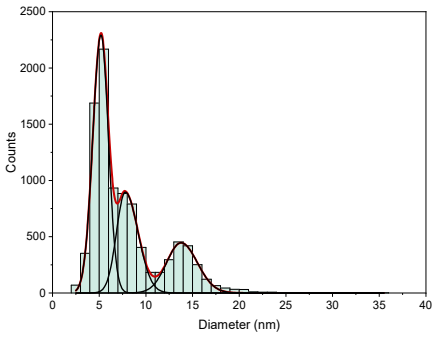	5.19 ± 0.66	7.79 ± 0.70	13.76 ±0.17
–70	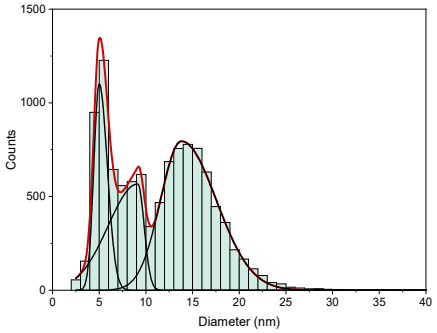	5.00 ± 0.05	9.14 ± 0.07	13.81 ± 0.12
–111	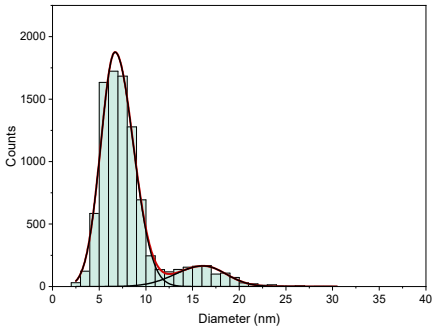	6.69 ± 0.14	16.16 ± 2.20	N/A

$V_{applied}$ (mV)	Distribution	Peak 1 (nm)	Peak 2 (nm)	Peak 3 (nm)
–140	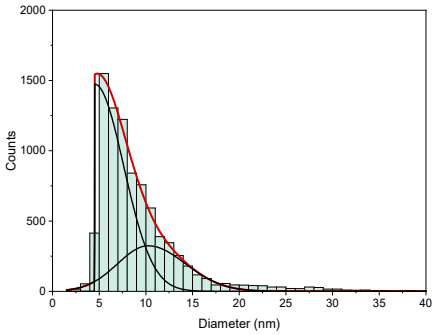	4.52 ± 0.47	10.23 ± 4.33	N/A
–160	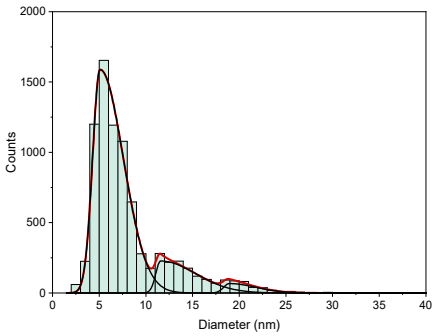	5.10 ± 0.06	11.59 ± 0.44	18.94 ± 1.13
–170	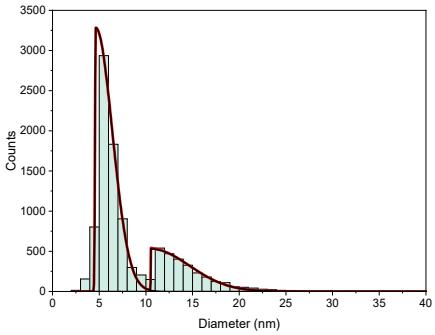	4.62 ± 0.21	10.52 ± 1.24	N/A
–180	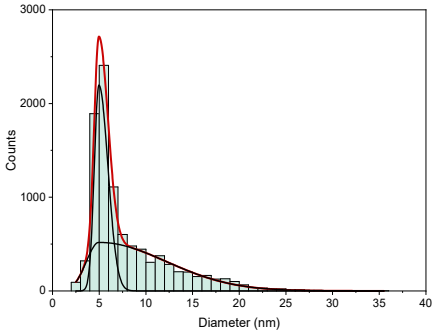	5.22 ± 0.03	9.19 ± 0.54	N/A

$V_{applied}$ (mV)	Distribution	Peak 1 (nm)	Peak 2 (nm)	Peak 3 (nm)
–200	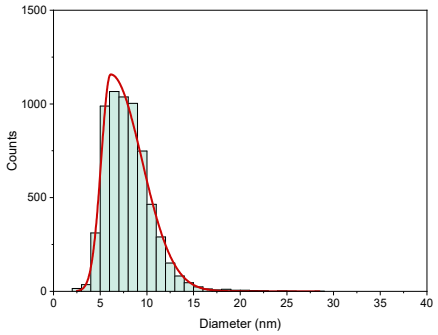	6.12 ± 0.09	N/A	N/A
–229	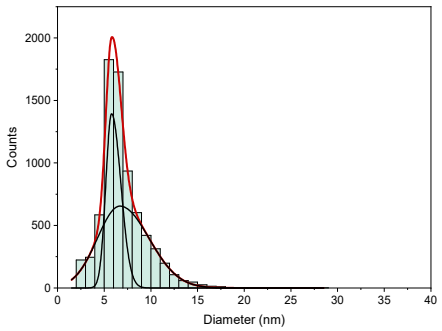	5.79 ± 0.03	6.68 ± 0.48	N/A
–270	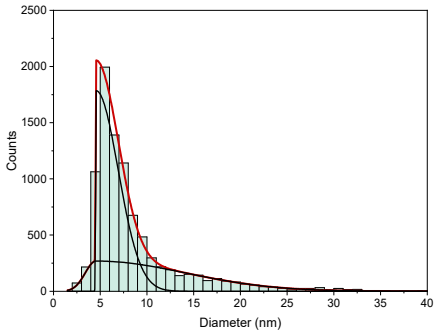	4.55 ± 0.41	4.55 ± 0.60	N/A
–670	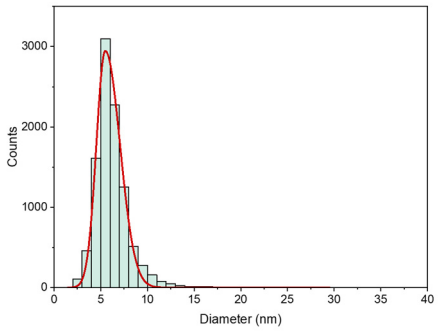	5.49 ± 0.09	N/A	N/A

$V_{applied}$ (mV)	Distribution	Peak 1 (nm)	Peak 2 (nm)	Peak 3 (nm)
–1170	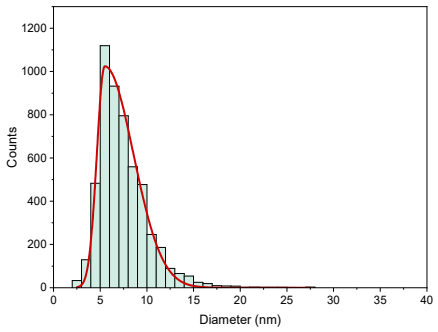	5.48 ± 0.18	N/A	N/A

*All experiments were run at 20% intensity, t_{pulse} = 1 s, and t_{rest} = 5 s. All values are reported with respect to the onset potential.

Table S3. Cu NPs Distribution for Varying Pulse Intensities.*				
Intensity (%)	Distribution	Peak 1 (nm)	Peak 2 (nm)	Peak 3 (nm)
10	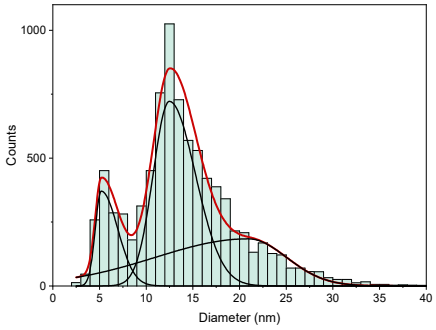	5.18 ± 0.69	12.48 ± 0.29	20.93 ± 2.74
20	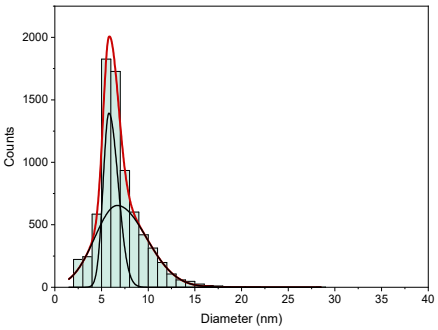	5.79 ± 0.03	6.68 ± 0.48	N/A
30	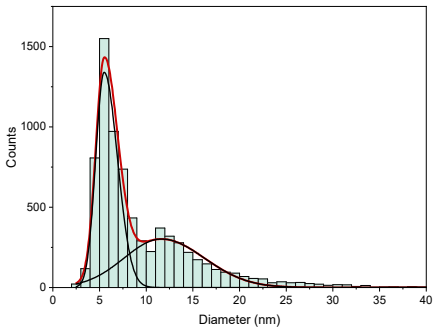	5.49 ± 0.13	11.62 ± 1.03	N/A
40	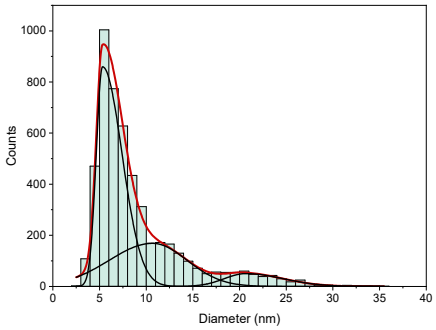	5.32 ± 0.20	10.68 ± 3.20	20.66 ± 2.43

Intensity (%)	Distribution	Peak 1 (nm)	Peak 2 (nm)	Peak 3 (nm)
50	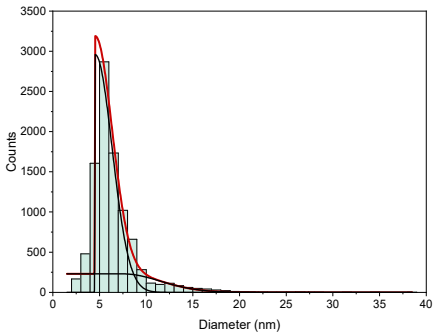	4.53 ± 0.63	7.44 ± 3.35	N/A
60	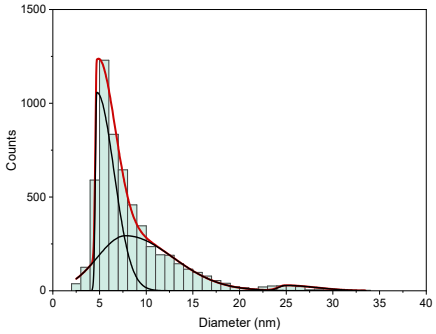	4.70 ± 0.57	7.78 ± 2.60	24.93 ± 2.26
70	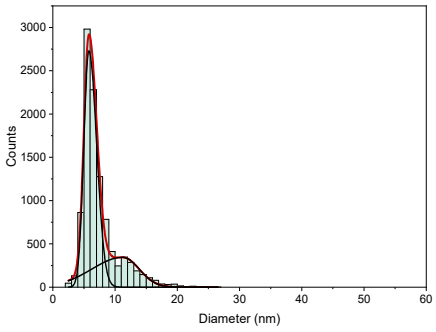	5.78 ± 0.10	11.23 ± 2.00	N/A

*All experiments were run at $V_{applied}$ = – 229 mV, t_{pulse} = 1 s, and t_{rest} = 5 s.

Table S4. Cu NPs Distribution for Varying Pulse Sequences.*						
t_{pulse} (s)	t_{rest} (s)	Distribution	Peak 1 (nm)	Peak 2 (nm)	Peak 3 (nm)	Peak 4 (nm)
0.1	0.5	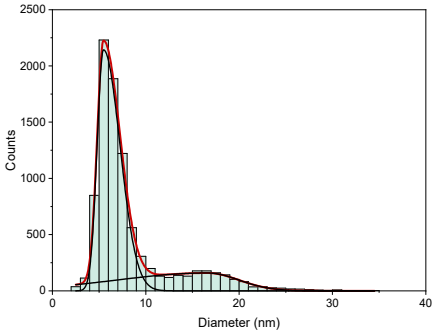	5.47 ± 0.05	16.58 ± 0.78	N/A	N/A
0.1	2.5	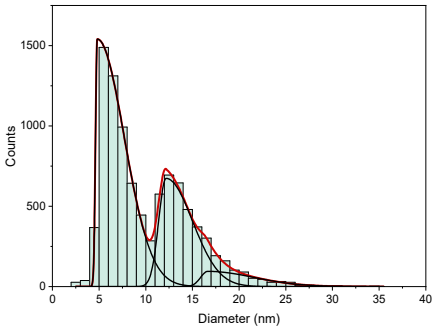	4.80 ± 0.22	12.18 ± 0.08	16.64 ± 0.68	N/A
0.1	5	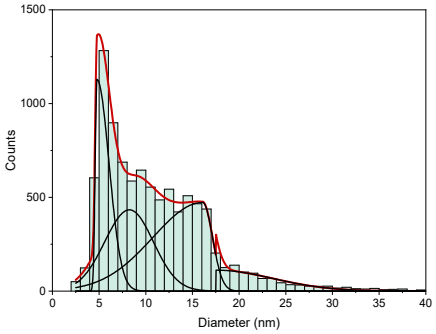	4.76 ± 0.75	8.26 ± 0.84	16.11 ± 0.22	17.50 ± 5.23

t_{pulse} (s)	t_{rest} (s)	Distribution	Peak 1 (nm)	Peak 2 (nm)	Peak 3 (nm)	Peak 4 (nm)
0.1	50	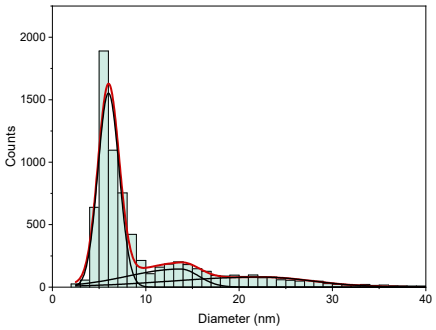	6.00 ± 0.15	13.72 ± 6.30	22.30 ± 11.95	N/A
0.5	0.5	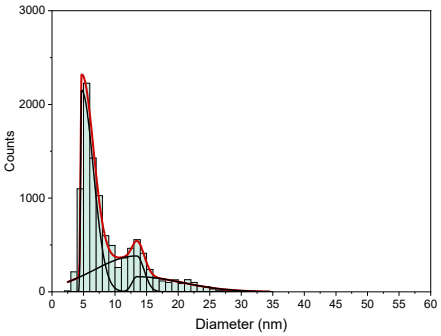	4.69 ± 0.53	13.45 ± 0.80	13.45 ± 2.61	N/A
0.5	2.5	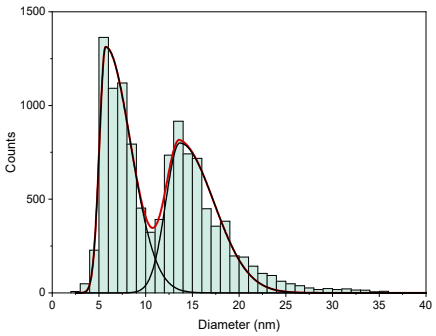	5.70 ± 0.12	13.64 ± 0.31	N/A	N/A

t_{pulse} (s)	t_{rest} (s)	Distribution	Peak 1 (nm)	Peak 2 (nm)	Peak 3 (nm)	Peak 4 (nm)
0.5	5	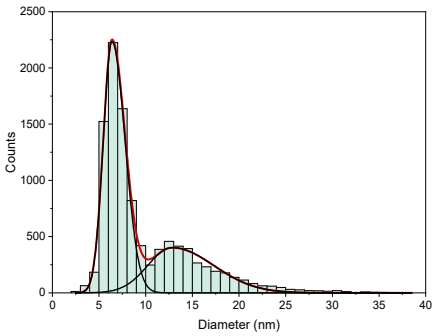	6.38 ± 0.62	12.83 ± 0.71	N/A	N/A
0.5	50	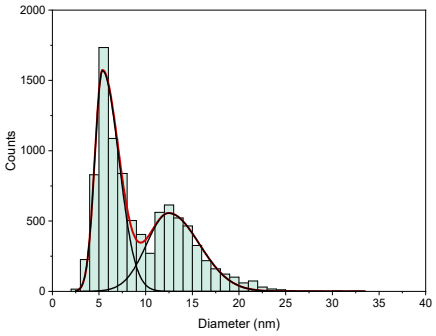	5.36 ± 0.18	12.46 ± 0.76	N/A	N/A
1	0.5	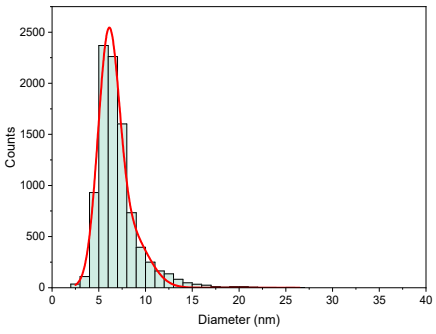	5.68 ± 0.09	N/A	N/A	N/A
1	2.5	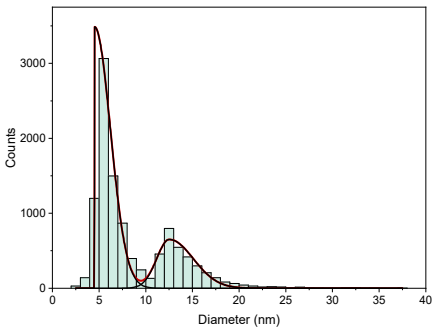	4.51 ± 0.61	12.51 ± 0.50	N/A	N/A

t_{pulse} (s)	t_{rest} (s)	Distribution	Peak 1 (nm)	Peak 2 (nm)	Peak 3 (nm)	Peak 4 (nm)
1	5	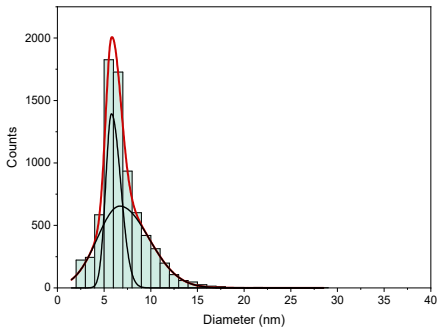	5.79 ± 0.03	6.68 ± 0.48	N/A	N/A
1	50	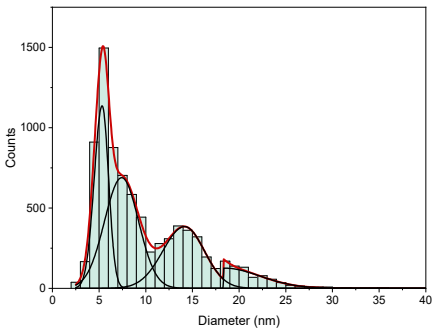	5.33 ± 0.05	7.42 ± 0.02	14.14 ± 0.21	18.34 ± 1.48
10	0.5	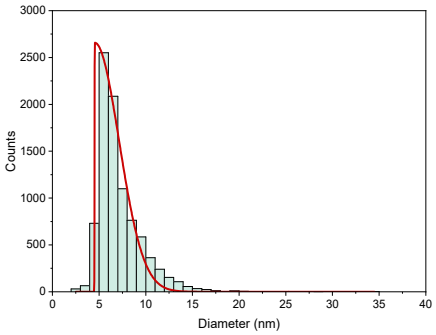	4.52 ± 0.60	N/A	N/A	N/A
10	2.5	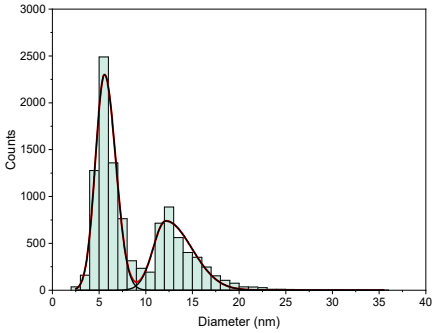	5.58 ± 0.16	12.14 ± 0.52	N/A	N/A

t_{pulse} (s)	t_{rest} (s)	Distribution	Peak 1 (nm)	Peak 2 (nm)	Peak 3 (nm)	Peak 4 (nm)
10	5	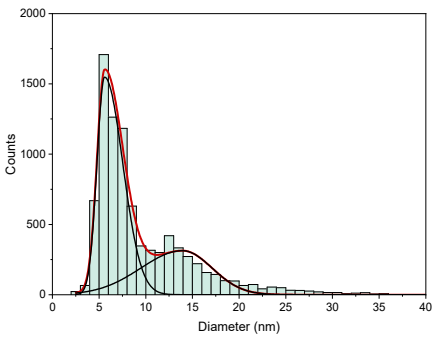	5.58 ± 0.12	13.94 ± 0.92	N/A	N/A
10	50	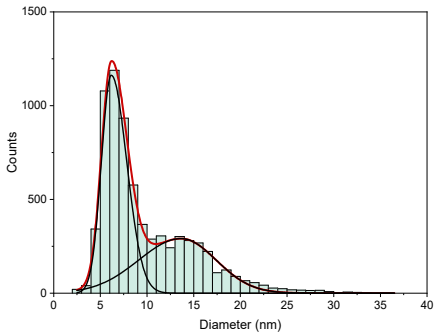	6.16 ± 0.07	13.65 ± 0.59	N/A	N/A

*All experiments were run at a 20% Intensity and $V_{applied}$ = – 229 mV.

Table S5. Cu NP Size Distribution for Varying Copper Oxidation Precursors.*				
Copper Salt (120 mM)	Distribution	Peak 1 (nm)	Peak 2 (nm)	Peak 3 (nm)
CuBr	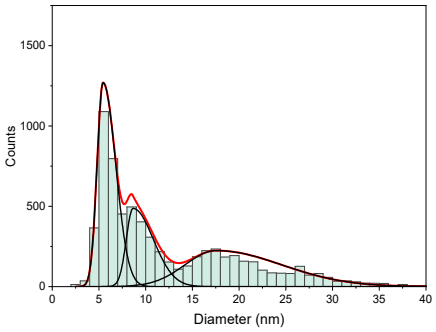	5.44 ± 0.41	8.64 ± 0.46	17.54 ± 1.00
$CuBr_2$	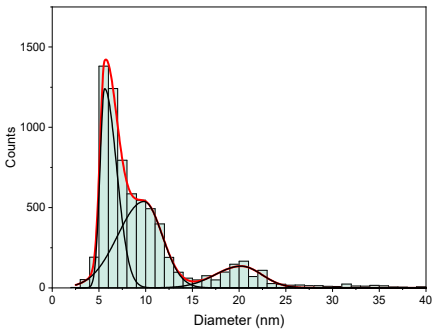	5.60 ±0.04	9.81 ± 0.20	20.22 ± 0.57

*all experiments were performed with the following conditions: $V_{applied}$ = –229 mV; 20% Intensity; t_{pulse} = 1 s; and t_{rest} = 2.5 s

References

1. Amatore, C.; Pfluger, F. *Organometallics.* 1990, **9**, 2276–2282.
2. Roberts, J. D.; Caserio, M. C., *Principles of Organic Chemistry*. W. A. Benjamin, Inc.: Menlo Park, CA, 1977.
3. Schumacher, J. E.; Hunt, H. *Ind. Eng. Chem.* 1942, **34**, 701–704.
4. Cifuentes, A.; Bernal, J. L.; Diez-Masa, J. C. *Anal. Chem.* 1997, **69**, 4271–4274.
5. Bagwe, R. P.; Khilar, K. C. *Langmuir.* 2000, **16**, 905–910.
6. Brust, M.; Walker, M.; Bethell, D.; Schiffrin, D. J.; Whyman, R. *J. Chem. Soc. Chem. Commun.* **1994,** 801–802.
7. Dadgostar, N.; Ferdous, S.; Henneke, D. *Mater. Lett.* 2010, **64**, 45–48.
8. Harris, D. C., *Quantitative Chemical Analysis*. 9th ed.; W. H. Freeman and Co.: New York, 2011.
9. Rahman, A.; Brown, C. W. *J. Appl. Polym. Sci.* 1983, **28**, 1331–1334.
10. Zhao, W.; Wang, Y. *Adv. Colloid Interface Sci.* 2017, **239**, 199–212.
11. Bard, A. J.; Faulkner, L. R., *Electrochemical Methods Fundamentals and Applications*. 2nd ed.; John Wiley & Sons, Inc.: New York, 2001.
12. Vieira, K. L.; Peters, D. G. *J. Electroanal. Chem. Interfac. Electrochem.* 1985, **196**, 93–104.
13. Open Circuit Potential. https://pineresearch.com/shop/kb/software/methods-and-techniques/basic-methods/open-circuit-potential-ocp/.
14. Greenbowe, T.; Meltzer, D. *Int. J. Sci. Educ.* 2003, **25**, 779–800.
15. Wadsö, L.; Li, X. *J. Chem. Educ.* 2008, **85**, 112.
16. Moulder, J. F.; Stickle, W. F.; Sobol, P. E.; Bomben, K. D., *Handbook of X-ray Photoelectron Spectroscopy*. Physical Electronics, Inc.: Eden Prairie, MN, 1995.
17. Goulet, P. J. G.; Leonardi, A.; Lennox, R. B. *J. Phys. Chem. C.* 2012, **116**, 14096–14102.